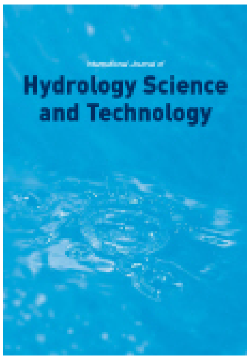

International Journal of Hydrology Science and Technology

ISSN online: 2042-7816 - ISSN print: 2042-7808
https://www.inderscience.com/ijhst

Analysing of rainfall-runoff modelling using a hybrid DNN-SGD optimisation in Sub Basin of Brahmaputra River, India

Subha Sinha

DOI: 10.1504/IJHST.2025.10067892

Article History:

Received:	20 February 2023
Last revised:	16 September 2023
Accepted:	12 November 2023
Published online:	03 December 2024

Analysing of rainfall-runoff modelling using a hybrid DNN-SGD optimisation in Sub Basin of Brahmaputra River, India

Subha Sinha

Department of Civil Engineering,
Bakhtiyapur College of Engineering,
Bakhtiyapur, India
and
Department of Science and Technology,
Government of Bihar, India
Email: starsubha@gmail.com

Abstract: The main objective of this research is to improve the accuracy of runoff prediction and assess the effectiveness of the proposed DNN-SGD model. The performance of the DNN-SGD model is evaluated using standard metrics, including the coefficient of determination (R^2), mean squared error (MSE), and root mean squared error (RMSE). The significance of findings demonstrating the superior performance of the proposed DNN-SGD model compared to other widely used methods, including ANN, DNN, ANN-PSO, and ANN-SGD. The results indicate that the DNN-SGD model achieved a remarkably high R^2 of 0.99998, indicating its ability to capture a large proportion of the variability in the observed data. Moreover, it obtained the lowest RMSE value of 0.002252 and MSE value of 0.000507, further confirming its superior accuracy and predictive capabilities. Overall, this study providing an advanced rainfall-runoff modelling approach for water resource management in the Brahmaputra River Sub Basin and other similar regions.

Keywords: rainfall; runoff; flood; deep neural network; DNN; stochastic gradient decent; SGD; Brahmaputra River; ANN PSO; water management; India.

Reference to this paper should be made as follows: Sinha, S. (2025) 'Analysing of rainfall-runoff modelling using a hybrid DNN-SGD optimisation in Sub Basin of Brahmaputra River, India', *Int. J. Hydrology Science and Technology*, Vol. 19, No. 1, pp.52–72.

Biographical notes: Subha Sinha is currently working as an Assistant Professor in Department of Civil Engineering, Bakhtiyapur College of Engineering, Bakhtiyapur, Department of Science and Technology, Government of Bihar, India.

1 Introduction

A surplus of storm water is present on the surface of the ground, and it does not penetrate into the soil. Runoff is made in manmade or natural ways. The runoff water is collected for productive use, known as water harvesting (Müller et al., 2020). Characteristics of rainfall such as distribution, duration and intensity, rainstorms and their presence can generate runoff (Kou et al., 2021; Liu et al., 2020; Sun et al., 2020). Due to the small amount of rainfall, water harvesting is difficult in zones of semi-arid and arid. Rainfall is used to calculate the runoff generation and examines the role of the degree of uncertainty (Adnan et al., 2021a). To determine the maximum rate of rainfall and its depth based on the copula multivariate function at various return rime. Using fuzzy set theory, determine the volume of runoff and flow of peak with its depth and rate of rainfall. The fuzzy-probabilistic model was used to establish an above 92% of flood in South Western Iran (Sabaghi et al., 2021).

To determine the surface runoff, the CN method was used. In China, gather the monitoring data of rainfall-runoff in 55 study areas. For runoff estimation, the CN method can lead to many errors. The revised CN method can reduce the error and determine the surface runoff volume. The rainfall runoff data was used to calculate the modified CN values (Lian et al., 2020). SWATgrid, HEC-HMS and IHACRES were compared and determined the relationship between rainfall and runoff. Under various climatic conditions, different couple catchment in Southeast Australia was validated and calibrated. Under hydro climatic conditions, runoff in the smaller catchment was determined by SWATgrid (Deb and Kiem, 2020). HEC-GeoHMS was used in the model of hydrological and checked the AI-Adhaim river catchment discharge by using GIS. The SCS-CN method was used to calculate routing, transport and loss. The coefficient of rainfall was determined and verified by the SCS-CN model. The final result indicates the corresponding model was suitable for the AI-Adhaim river catchment (Hamdan et al., 2021).

The hydro-meteorological methods SCS-CN and HEC-HMS have been used in existing studies (Ben Khélifa and Mosbahi, 2021; Elagca, 2022; Ibrahim et al., 2021; Chiang et al., 2022; Gholami and Khaleghi, 2021; Bunganaen et al., 2021; Faouzi et al., 2022; Kumar and Sherring, 2021). In recent days, methods of neural networking (NN) have been used for predicting rainfall runoff. Because this NN model saves a lot of time and is a quick method compared to hydrological methods, it always develops the results. The main advantage of the NN is that it is multitasking and gives the best results and performance compared to hydrological methods. LSTM is one of the NN models used to overcome the NN traditional models. This study investigates the effects of hysteresis and determines ML methods' performance. The final results indicate the artificial neural networks (ANN) give better results with LSTM than traditional methods. Using LSTM increased root mean squared error (RMSE) by 27%. ML was used for hydrological modelling (Mao et al., 2021). The combination of EANN-GA was used for determining the rainfall runoff and compared to ANN and EANN. The performance of EANN-GA is better than the EANN model by 35% and 19% in terms of test fit criteria for Murrumbidgee and Aji Chai catchment catchments (Molajou et al., 2021).

For the simulation of forecast and flood, PSO-LSTM was used. The hyperparameters of LSTM were optimised by protocol. The result showed the changes in hyperparameters caused by LSTM. The optimisation of hyperparameters gave better results and was compared with NN models (Xu et al., 2022). Rainfall-runoff modelling was done by an ANN, and the infiltration was determined based on different land use. During the modelling process, an initial loss is made, and it indicates the final result (Gholami and Sahour, 2022). Jimmy et al. (2021) predicted the runoff by FFBPN, ANFIS and NMR in the Thiruvananthapuram watershed, Kerala. In this study, the output of the runoff is taken by the inputs such as temperature, ET loss, loss of infiltration and precipitation. The result of the study was obtained by ANNs. R^2 and RMSE were determined by this study. From the ANNs techniques, ANFIS gives better performance than NMR and FFBPNN.

Adnan et al. (021b) proposed a rainfall runoff modelling using M5Tree, ANFIS-FCM, ANFIS-PSO and MARS with the MM-SA method. In this study, the Samoggia river basin was selected for modelling rainfall-runoff. AIA, scatter index, RMSE, and NSE are calculated by capability methods. When comparing the M5Tree model MARS, ANFIS-PSO and ANFIS-FCM models gave better accuracy data. RMSE values of MARS, M5Tree, ANFIS-PSO and ANFIS-FCM were 7.4%, 28.8%, 8.5% and 5%, respectively. In some cases, the performance of ML methods was best than MARS and M5Tree models. Simulation of rainfall-runoff was proposed by Okkan et al. (2021) using the ML technique with a conceptual model. The output data was determined by a nested hybrid model in the Gediz river basin, Turkey. The output performance of the nested hybrid model was better than standalone and coupled models. In this study, the parameters were calibrated, and the output to simulate monthly runoff was examined.

Nourani et al. (2021) proposed modelling of rainfall-runoff using gauge rainfall data input fusion and MSS. In the Gilgel Abay catchment, Ethiopia, the rainfall runoff modelling was done by SVR, ANFIS and FFNN models. Nonlinear analysis was used to select the input parameters. Two stages were conducted in this study, the input parameters were trained in the first stage, and the second stage was NNE, WA, and SA were used to conduct the runoff modelling. The performance of the NNE method was more developed than other methods. The accurate performance was given as a final result by ensemble modelling. The proposed rainfall runoff modelling was done by Sezen and Partal (2022) using a hybrid GR6J-WGANN approach. In this study, the performance of runoff was calculated by the GR6J-WGANN approach in the Konya closed basin, Turkey. Rainfall-runoff was improved by GR6J-WGANN1, GR6J and GR6J-WGANN2.

Based on the existing studies, several research gaps can be identified. Most of the studies focus on different regions. There is a gap in research that specifically addresses rainfall-runoff modelling in the Brahmaputra River basin. While some studies have explored the use of traditional hydrological methods, there is a need to investigate the application of advanced modelling techniques with use of optimisation algorithm in the situation of rainfall-runoff modelling in this region. Research should focus on the impacts on runoff in the Brahmaputra River basin, which is essential for flood forecasting and management. Focusing on these research gaps can contribute to the development of rainfall-runoff models in the Brahmaputra River sub-basin. These models are critical for improving water resource management and enhancing disaster preparedness in the region. Therefore this study aims to develop a novel hybrid deep neural network-stochastic gradient decent (DNN-SGD) optimisation for predicting the runoff in the Sub Basin (Brahmaputra lower) of the Brahmaputra River, India.

The problem of accurately modelling rainfall-runoff processes is importance in hydrology and water resource management. Reliable runoff models are crucial for flood forecasting, water resource allocation, and disaster preparedness. Traditional hydrological models have limitations in capturing the complex and dynamic nature of rainfall-runoff relationships, especially in regions prone to extreme weather events like the Brahmaputra River basin in India. There is a need for advanced modelling techniques to enhance the accuracy of runoff predictions in this region.

The Brahmaputra River basin was selected for this study due to several reasons. The Brahmaputra River is one of the major rivers in the world and plays a vital role in the socio-economic and environmental aspects of the region. It is crucial to have accurate rainfall-runoff models for such a significant river basin. The Brahmaputra River basin is susceptible to extreme weather events, including heavy monsoon rains and flooding. Accurate rainfall-runoff modelling is essential for timely flood forecasting and mitigation, which can save lives and reduce property damage. The Brahmaputra River is a vital source of water for agriculture, industry, and domestic use in the region. Precise runoff predictions are necessary for sustainable water resource management and allocation, especially as water demand continues to increase. The availability of long-term precipitation data for this specific region (2001–2021) allows for a comprehensive analysis of historical rainfall patterns.

The selection of a hybrid DNN combined with SGD optimisation is motivated by several factors. Rainfall-runoff relationships are highly complex and nonlinear. DNNs are well-suited to capture these complex patterns, making them a promising choice. SGD is known for efficiently optimising DNNs. The combination of DNN with SGD can enhance the model's training speed and convergence. The novelty of this study lies in the integration of a DNN-SGD hybrid model to challenge the complex problem of rainfall-runoff modelling in the Brahmaputra River sub-basin. While DNNs have been applied in hydrology, the use of SGD optimisation in this perspective, especially for this specific region, is less explored. Additionally, the focus on a 20-year dataset for a region prone to climatic variability adds a novel dimension to the study, allowing for a comprehensive understanding of long-term trends and variations in runoff dynamics in the Brahmaputra River sub-basin. The following are the objectives of the present study,

- To develop a rainfall-runoff model in the Brahmaputra River based on weather data.
- To combine DNNs with SGD to improve the accuracy of runoff prediction.
- To evaluate the performance of the DNN-SGD model using standard metrics, including R^2, mean squared error (MSE), and RMSE.
- To assess the effectiveness of the proposed DNN-SGD model compared to other existing methods.

The proposed methodology is given in Section 2, the study area and methods are given in Sections 2.1 and 2.2, respectively, Section 3 explains the result and discussion, and finally, the conclusion is given in Section 4, which follows below.

2 Data collection and methodology

2.1 Proposed methodology

The proposed methodology for this study is as follows: the study area encompasses the Sub Basin of Brahmaputra River in India. Precipitation data covering from the year 2001 to 2021 is collected for this region (NASA, 2021). The collected data is then preprocessed to handle missing values, outliers, and ensure data consistency. A DNN is designed and configured to capture the complex relationships between precipitation and runoff. SGD is employed as the optimisation algorithm to efficiently train the DNN. The DNN-SGD model is trained using the prepared precipitation data. The performance of the DNN-SGD model is assessed using standard metrics, including the R^2, MSE, and RMSE. The performance of the DNN-SGD model is compared with several baseline models, including traditional ANN, DNN, artificial neural networks with particle swarm optimisation (ANN-PSO), and ANN with SGD. The findings of the study are discussed. The conclusion summarises the outcomes recommendations provided for further research. Figure 1 shows the layout of the proposed work.

Figure 1 Layout of proposed work (see online version for colours)

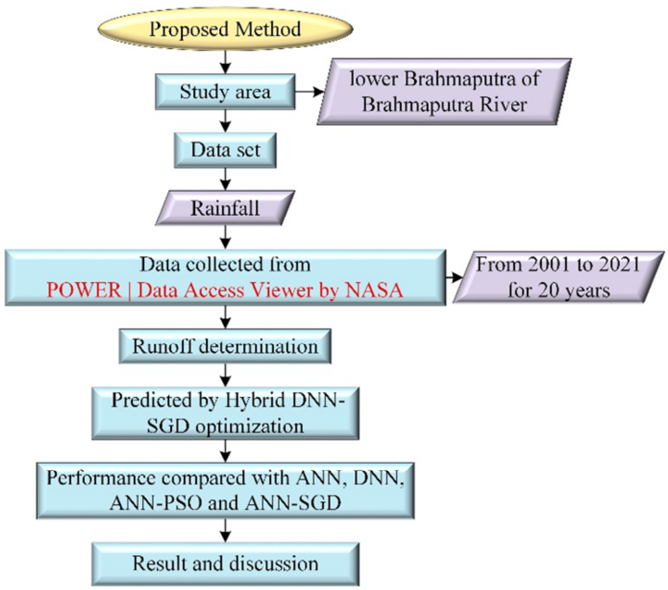

2.2 Study area description

In this study, the Sub Basin of Brahmaputra River (Brahmaputra lower) was chosen for an experimental site, the main river of Assam state (Tsering et al., 2021). The distance across the Brahmaputra River is above 80km, the length of the river is 2,900 km, and the elevation is 5,300 m (Barbulescu et al., 2021; Suresh et al., 2022). Brahmaputra River catchment is 293,000 sq.km in Tibet, 47,000 sq.km in Bangladesh and 2, 40,000 sq.km in Bhutan and India. Above 20,000 cumec is a typical discharge per annum (Ahmed et al., 2021; Dietrich et al., 2020; Rao et al., 2020). The minimum and maximum discharge of the Brahmaputra River is 1,757 cumec and 72.779 cumec. This river is one of the major rivers in the world. In India, most of the rivers are known as the Female River, but the Brahmaputra is known as the Male River. The climatic condition of the Brahmaputra River is in Tibet dry and cold conditions, humid and warm in Bangladesh and Assam, and flood is the general incident in the monsoon season (Wang et al., 2020; Liu et al., 2020). Heavy drops of rain are the main reason for the river overflowing. During the monsoon season, there are massive amounts of rainfall that increase the volume of water and cause runoff. Figure 2 shows the location of the Sub Basin (Brahmaputra lower) of the Brahmaputra River, India.

Figure 2 Location of the study area (see online version for colours)

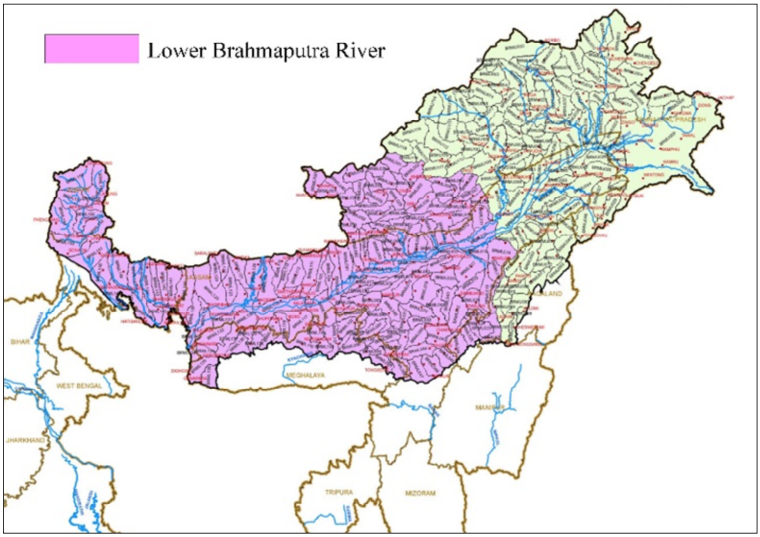

Table 1 Collected weather parameter

Year	*Precipitation (rainfall) mm/day*
2001	5.18
2002	6.22
2003	5.62
2004	6.44
2005	6.24
2006	4.4
2007	5.23
2008	4.72
2009	5.61
2010	5.86
2011	5.29
2012	5.35
2013	5.1
2014	4.7
2015	5.59
2016	6.71
2017	7.33
2018	5.88
2019	7.95
2020	9.14
2021	5.96

Source: NASA (2021)

2.3 Data used

In this study, the input parameter data, like precipitation is used to predict the runoff, and the collected weather data is given in Table 1. Data on precipitation for the period from 2001 to 2021 has been gathered for the Sub Basin of the Brahmaputra River region (NASA, 2021). In this present study, predict the runoff by DNN-SGD optimisation yearly scale data and determine the R^2, RMSE and MSE for yearly scale data and find out the best performance of the model. Compare the yearly scale performance with DNN, ANN, ANN-PSO and ANN-SGD.

2.4 Techniques used

Recently, NN methods have been used for predicting the runoff. Because this NN model saves a lot of time and is a quick method compared to hydrological methods, it always develops the results, and the main advantage of the NN is that it is multitasking and gives the best results and performance compared to hydrological methods. This study used a hybrid DNN-SGD optimisation to analyse the rainfall-runoff using weather data.

2.4.1 Deep learning neural network

Feed forward neural networks (FFNNs) are the other name for DNN. In the DNN technique, the data run only forward trend and do not run towards the back (Chen et al., 2021). DNN consists of three layers: input, output and hidden. In the DNN technique, more than two hidden layers are present in the structure (Xue et al., 2020) The input precipitation data are specified in input layers, and a variety of neurons are in hidden layers. Weight optimisation in hidden layers and getting the output data from the output layer. From this, model performance of runoff is determined. The process of DNN was done by transferring one neuron to another neuron. Figure 3 indicates the structure of DNN.

This study employs SGD optimisation to enhance the model's performance by optimising its weights. SGD is a widely used optimisation algorithm in machine learning and deep learning. It helps train different models effectively. The variant of the gradient descent algorithm is called stochastic gradient descent (SGD). It updates model parameters iteratively, relying on individual training samples, not the entire dataset. SGD's main concept involves updating model parameters using randomly sampled data points from the training dataset. This helps approximate the true gradient of the cost function by considering one data point at a time. Compared to standard gradient descent, SGD can achieve faster convergence, especially with large datasets. SGD's randomness acts as implicit regularisation, preventing overfitting to training data. In contrast to batch gradient descent, SGD only requires one sample in memory per iteration, making it memory-efficient for large datasets. SGD serves as an initial optimisation algorithm and supports advanced techniques like Adam, RMSprop, and Adagrad. In contrast, SGD updates parameters for each training example, $x^{(i)}$ and its corresponding label, $y^{(i)}$ expressed in equation (1) (Ruder, 2016). Figure 4 shows the flowchart for the hybrid DNN-SGD algorithm for runoff prediction.

$$\rho = \rho - \upsilon.\nabla_{\rho} J\left(\rho; x^{(i)}; y^{(i)}\right) \tag{1}$$

Figure 3 DNN structure (see online version for colours)

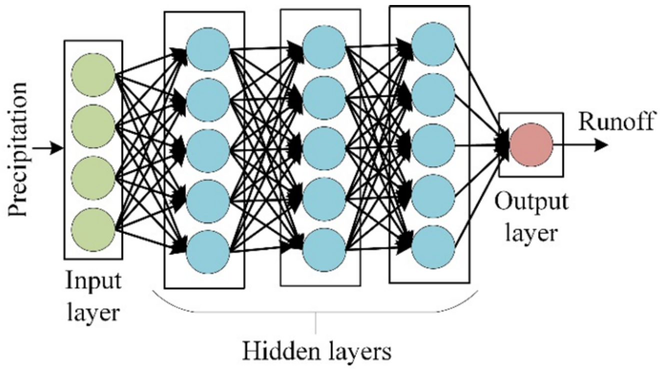

2.4.1.1 Training and testing phases

In this study, runoff prediction has been made using DNN-SGD optimisation. The dataset has been divided into training and testing sets with a split of 80% for training and 20% for testing. The training phase involves data preparation, data splitting, input-output pairing, DNN-SGD optimisation, training the model, and evaluating its performance. On the other hand, the testing phase comprises data evaluation, calculating prediction errors, and using performance metrics to assess the model's accuracy.

During the training phase, weather parameter data was used that are collected from 2001 to 2021, which included precipitation values in mm/day. Then, the runoff was calculated using equation (2). Next, the dataset was divided into training and testing sets, with 80% allocated for training and 20% for testing the model's performance. For training, the precipitation values were paired as inputs with their corresponding calculated runoff values as outputs. To train the DNN model, the DNN-SGD optimisation technique was employed to defining the network architecture, selecting appropriate activation functions, optimiser, and loss function. The model was trained on the training dataset, with its parameters iteratively adjusted using SGD to minimise prediction error. Throughout the training process, the model's performance was monitored using metrics like R^2, MSE and RMSE on the training set to ensure its accuracy and generalisation.

In the testing phase, the trained DNN-SGD model was applied to predict runoff values for the testing dataset, which contained the 20% of data set aside earlier for evaluation. Then compared these predicted runoff values with the actual runoff values from the testing dataset to measure the model's performance. To quantify the model's accuracy and generalisation capability, evaluation metrics were used such R^2, MSE and RMSE to assess the prediction errors. Furthermore, in this phase, the performances of different models, including ANN, ANN-PSO, ANN-SGD and DNN compared with proposed model.

Figure 4 Flowchart for the hybrid DNN-SGD algorithm for runoff prediction

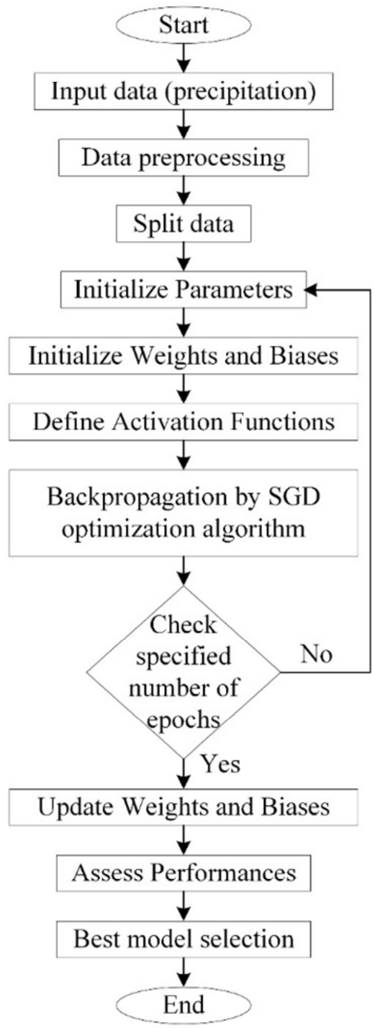

2.4.2 Artificial neural network

From biological neural networks, the term ANN is derived and is related to the human brain. The ANN structure has neurons which are also known as nodes. ANN consists of multiple artificial neurons and is arranged in a series of layers consisting of three layers: input, hidden and output, shown in Figure 5. The following is the working process of the ANN technique. The inputs are assigned to input layers, and then the input is multiplied by its equivalent weights. These weighted inputs are summarised, and the activation function achieves the output.

Figure 5 ANN structure (see online version for colours)

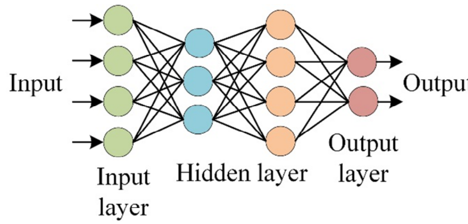

2.5 Runoff determination

The surface runoff is calculated by a direct formula, which is an uncomplicated method. The runoff is determined by multiplying the area with rainfall and dividing by 231. Runoff is denoted by *Q*, the unit is in3/day, and equation (2) shows the determination of runoff.

$$Runoff\ Q = \frac{AI}{231} \tag{2}$$

where *A* is the area of the study region, *I* rainfall data and *Q* is the observed runoff.

2.6 Evaluation criteria

The coefficient of determination (R^2), MSE and RMSE were used to determine the exactness of the DNN-SGD technique. In this study, R^2, RMSE and MSE values were examined to determine the performance and effectiveness of the model. These are the important steps in the machine learning model, and the following equations (3) to (5) are used to find the R^2, RMSE and MSE. The highest R^2 and lowest MSE and RMSE indicate the best performance of the model.

2.6.1 Coefficient of determination (R^2)

The coefficient of determination, often denoted as R^2, is a statistical measure that represents the proportion of variance in the dependent variable (target) that is predictable from the independent variables (features) in a regression model. It is a value between 0 and 1, where 1 indicates a perfect fit.

$$R^2 = 1 - \frac{\sum \left(x_i - x_j\right)^2}{\sum \left(x_i - x_k\right)^2} \tag{3}$$

2.6.2 Mean squared error

The MSE is a commonly used metric to evaluate the accuracy of a regression model. It measures the average squared difference between the predicted values and the actual values. A lower MSE value indicates better performance, as it means that the model's predictions are closer to the actual values.

$$MSE = \frac{1}{K}\sum_{i=1}^{K}\left(x_i - x_j\right)^2 \tag{4}$$

2.6.3 Root mean squared error

The RMSE is derived from the MSE and is widely used in regression tasks. It is the square root of the MSE and is in the same unit as the target variable, making it more interpretable than MSE. Like MSE, a lower RMSE value indicates better performance, and it measures the average distance between the predicted and actual values.

$$\sqrt{MSE} = RMSE = \sqrt{\frac{1}{K}\sum_{i=1}^{K}\left(x_i - x_j\right)^2} \tag{5}$$

where x_i is observed value, x_j is simulated value, x_k is average observed value, K is total number of data point in the data set.

3 Result and discussion

In this study, the first runoff is determined by precipitation data and predicted by DNN-SGD optimisation. In addition, each method's performances were determined and all methods' performance were compared to identify better performance.

3.1 Enhanced runoff prediction performance with DNN-SGD optimisation

Figure 6 shows the runoff prediction performance of different methods using various optimisation techniques. A correlation coefficient close to 1 indicates a strong linear relationship between the predicted runoff and the actual runoff values. The simple ANN approach yielded a correlation coefficient of 0.95641, which is significantly lower than the proposed method. The lower correlation might be due to limitations in the ANN's architecture or hyperparameters. This suggests that the basic ANN model not capturing the underlying patterns in the runoff data as effectively as the proposed DNN-SGD method. By incorporating particle swarm optimisation (PSO) to tune the ANN's parameters, the correlation coefficient improved to 0.97739. Although PSO is a strong optimisation technique, it is not as effective as the proposed DNN-SGD method. This suggests that PSO can improve ANN models but not be as good as SGD optimisation in this case.

Using SGD optimisation for the ANN yielded a higher correlation coefficient of 0.98589 compared to the ANN without optimisation. This shows the significance of SGD in improving the ANN's performance. However, it still did not outperform the proposed DNN-SGD method. The DNN model without any optimisation achieved a correlation coefficient of 0.98951, which is already quite high. The DNN architecture shows significant predictive power, yet it falls short of the accuracy achieved by the proposed DNN-SGD method, suggesting that SGD optimisation provides an additional performance boost.

When compared to other predictive models, the proposed DNN-SGD optimisation model achieved the highest correlation coefficient (R) of 0.99998, which provides excellent prediction accuracy. The use of SGD optimisation in combination with DNN potential contributed to its superior performance. SGD enables the model to efficiently find the optimal weights and biases during the training process, leading to better performances. The other methods, such as basic ANN, ANN-PSO, ANN-SGD, and DNN without optimisation, also show decent predictive capabilities with correlation coefficients ranging from 0.95641 to 0.98951. These results indicate that both traditional ANN models and deep learning-based DNN models can provide reasonably accurate runoff predictions. In this case, SGD optimisation seems to be particularly well-suited for enhancing the performance of DNN models in runoff prediction.

Figure 6 Observed runoff vs. predicted runoff by DNN-SGD, ANN, DNN, ANN-PSO and ANN-SGD (see online version for colours)

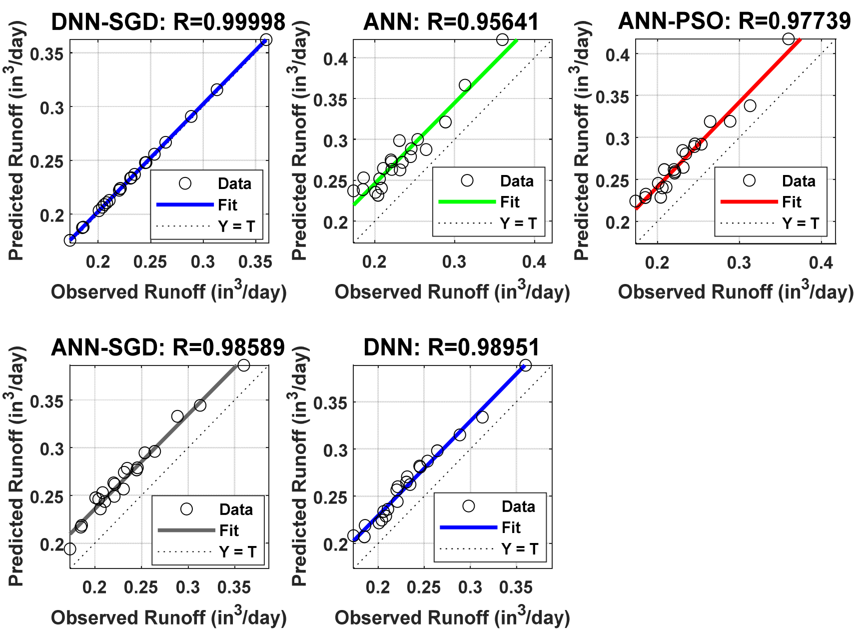

3.2 *Rainfall-runoff prediction performance analysis*

The performance of the input model based on multiple scoring conditions was evaluated at the annual scale, with a focus on precipitation. A variety of transfer functions, including logarithmic sigmoidal, Purelin, and tangential sigmoidal, are grouped together in different architectures to ensure the efficiency and performance of the model. Testing values of R^2, RMSE and MSE were determined which are commonly used to assess the accuracy and predictive capabilities of models. The performance results for various methods, including ANN, ANN-PSO, ANN-SGD, DNN, and DNN-SGD presented in Tables 2–6.

Table 2 Prediction performance by ANN

Input model	*MSE*	*RMSE*	*R^2*
Precipitation (2001–2021)	6.56E-06	0.0026	0.8805
	8.31E-06	0.0029	0.8779
	7.12E-06	0.0027	0.8404
	4.80E-06	0.0022	0.8454
	5.61E-06	0.0024	0.8514
	6.06E-06	0.0025	0.7309
	8.89E-06	0.003	0.8177
	4.65E-06	0.0022	0.7345
	8.15E-06	0.0029	0.8098
	6.99E-06	0.0026	0.7727
	5.65E-06	0.0024	0.8667
	4.80E-06	0.0022	0.7965
	5.90E-06	0.0024	0.8535
	6.16E-06	0.0025	0.7754
	4.50E-06	0.0021	0.8008
	6.71E-06	*0.0026*	*0.9186*
	4.96E-06	0.0022	0.8981
	5.69E-06	0.0024	0.8812
	6.67E-06	0.0026	0.8543
	5.07E-06	0.0023	0.8526
	0.001386	0.0372	0.8631

Table 3 Prediction performance by ANN-PSO

Input model	*MSE*	*RMSE*	*R^2*
	0.7951	0.8917	0.9443
	0.7171	0.8468	0.9202
	0.7283	0.8534	0.9238
	0.7545	0.8686	0.932
	0.7071	0.8409	0.917
	0.5978	0.7732	0.8793
	0.7366	0.8582	0.9264
	0.6399	0.7999	0.8944
	0.7356	0.8577	0.9261
	0.6581	0.8113	0.9007
	0.6339	0.7962	0.8923
	0.7646	0.8744	0.9351
	0.6699	0.8185	0.9047
	0.6568	0.8104	0.9002

Table 3 Prediction performance by ANN-PSO (continued)

Input model	*MSE*	*RMSE*	*R^2*
	0.7072	0.8409	0.917
	0.6859	0.8282	0.9101
	0.8175	0.9042	0.9509
	0.7676	0.8762	0.936
	0.8587	*0.9267*	*0.9626*
	0.7431	0.862	0.9285

Table 4 Prediction performance by ANN-SGD

Input model	*MSE*	*RMSE*	*R^2*
Precipitation (2001–2021)	0.6871	0.8289	0.9105
	0.7831	0.8849	0.9407
	0.7145	0.8453	0.9194
	0.7404	0.8604	0.9276
	0.7757	0.8807	0.9385
	0.7988	0.8938	0.9454
	0.7623	0.8731	0.9344
	0.7229	0.8502	0.9221
	0.787	0.8871	0.9419
	0.8083	0.899	0.9482
	0.6781	0.8235	0.9074
	0.7481	0.8649	0.93
	0.6586	0.8115	0.9008
	0.7286	0.8536	0.9239
	0.6994	0.8363	0.9145
	0.7961	0.8922	0.9446
	0.7518	0.867	0.9311
	0.713	0.8444	0.9189
	0.8263	0.909	0.9534
	0.8676	*0.9315*	*0.9651*
	0.7106	0.843	0.9181

Table 5 Prediction performance by DNN

Input model	*MSE*	*RMSE*	*R^2*
Precipitation (2001–2021)	0.8241	0.9078	0.9528
	0.7548	0.8688	0.9321
	0.7245	0.8512	0.9226
	0.7798	0.8831	0.9397
	0.7653	0.8748	0.9353
	0.693	0.8325	0.9124

Table 5 Prediction performance by DNN (continued)

Input model	*MSE*	*RMSE*	*R^2*
Precipitation (2001–2021)	0.7759	0.8809	0.9386
	0.7204	0.8488	0.9213
	0.8174	0.9041	0.9508
	0.7589	0.8712	0.9334
	0.8278	0.9098	0.9539
	0.7954	0.8919	0.9444
	0.8202	0.9056	0.9516
	0.7992	0.894	0.9455
	0.7359	0.8578	0.9262
	0.7855	0.8863	0.9414
	0.8397	0.9164	0.9573
	0.7324	0.8558	0.9251
	0.8798	*0.938*	*0.9685*
	0.8574	0.926	0.9623
	0.8004	0.8946	0.9459

Table 6 Prediction performance by proposed DNN-SGD

Input model	*MSE*	*RMSE*	*R^2*
Precipitation (2001–2021)	0.000655	0.002561	0.9876
	0.00083	0.002882	0.9884
	0.00071	0.002669	0.9881
	0.000479	0.00219	0.9914
	0.000561	0.002369	0.9904
	0.000605	0.002461	0.986
	0.000889	0.002982	0.9857
	0.000465	0.002156	0.9885
	0.000815	0.002856	0.9872
	0.000699	0.002645	0.9887
	0.000564	0.002376	0.9887
	0.00048	0.002191	0.9897
	0.000589	0.002428	0.9881
	0.000616	0.002482	0.9868
	0.000449	0.002121	0.9905
	0.00067	0.00259	0.9903
	0.000495	0.002226	0.9923
	0.000568	0.002385	0.9898
	0.000667	0.002583	0.9918
	0.000507	*0.002252*	*0.9938*
	0.000524	0.00229	0.9903

For the ANN method, the testing values of MSE, RMSE, and R^2 were found to be 6.71E-06, 0.0026, and 0.9186, respectively. Meanwhile, the performance testing values for ANN-PSO were 0.8587, 0.9267, and 0.9626 for MSE, RMSE, and R^2, respectively. On the other hand, ANN-SGD demonstrated R^2, RMSE, and MSE values of 0.9651, 0.9315, and 0.8676, respectively. The DNN method yielded an R^2 value of 0.9685, RMSE of 0.938, and MSE of 0.8798. The DNN-SGD optimisation method emerged as the best-performing approach, surpassing all other methods in terms of predictive accuracy. It delivered superior R^2, RMSE, and MSE values compared to ANN, ANN-PSO, ANN-SGD, and DNN methods, demonstrating its effectiveness in predicting precipitation at the annual scale. The detailed discussion is provided in the following section.

3.2.1 Comparative analysis of prediction models

Table 7 presents a performance comparison of different methods using various evaluation metrics, including MSE, RMSE, and R^2. From Table 7, the ANN achieved a very low MSE and RMSE, indicating that it is good at minimising prediction errors. However, the R^2 value of 0.9186 suggests that the model explains approximately 91.86% of the variance in the data. The 0.9626 R^2 value from ANN-PSO indicates that this model explains 96.26% of the variance, showing better performance than the basic ANN.

Like ANN-PSO, ANN-SGD also shows higher MSE and RMSE compared to the basic ANN, suggesting that SGD not have been as effective for this particular dataset. However, the R^2 value of 0.9651 indicates that this model explains 96.51% of the variance, performing slightly better than ANN-PSO. The R^2 value of 0.9685 from DNN shows that this model explains 96.85% of the variance, which is better than both ANN-PSO and ANN-SGD in terms of explained variance. When compared to other models, proposed DNN-SGD model appears to be a novel approach that combines the complexity of a DNN with the optimisation power of SGD. The significantly lower MSE and RMSE values suggest that DNN-SGD model can make more accurate predictions. The high R^2 value of 0.9938 indicates an exceptional level of explanation (99.38%) of the variance in the data, making it the best-performing model among ANN, DNN, ANN-PSO and ANN-SGD.

Table 7 Performance comparison

Methods	*MSE*	*RMSE*	*R^2*
ANN	6.71E-06	0.0026	0.9186
ANN-PSO	0.8587	0.9267	0.9626
ANN-SGD	0.8676	0.9315	0.9651
DNN	0.8798	0.938	0.9685
Proposed DNN-SGD	*0.000507*	*0.002252*	*0.9938*

From the results, the comparison methods like ANN, DNN, ANN-PSO and ANN-SGD not efficient in finding the optimal parameters for the prediction. The proposed DNN-SGD performs better with the highest R^2 of 0.9938, the lowest RMSE value of 0.002252, and the MSE value of 0.000507. The proposed method utilises SGD as its optimisation algorithm. SGD is a widely used and powerful optimisation technique in deep learning, capable of finding good parameter values by updating them iteratively based on the gradients of the loss function. It can lead to better results and contribute to its superior performance.

3.3 Performance comparison of rainfall-runoff models: DNN-SGD vs. ANN, ANN-PSO, ANN-SGD, and DNN

Figure 7 shows the comparison of the predicted runoff by the proposed model (DNN-SGD) with other comparison models (ANN, ANN-PSO, ANN-SGD, DNN), for the years 2001 to 2021. The data represents runoff predictions and actual runoff values for the years 2001 to 2021. The X-axis represents the years, and the Y-axis represents the predicted runoff values for each year. The ANN model generally performs well, but it has slightly larger deviations from the actual values compared to the proposed model. In ANN-PSO model, PSO is used to train the ANN. The predictions are close to the actual values, but this model also have slightly larger errors than the proposed model. ANN-SGD model uses SGD to train the ANN and the performance is similar to the standard ANN, but it have slightly larger errors compared to the proposed model. The DNN model provides predictions with moderate accuracy, but it shows little deviations from the actual values compared to the proposed DNN-SGD model. The predicted runoff values from the DNN-SGD model closely align with the actual runoff values for all the years, demonstrating its accuracy in capturing the variations in the runoff patterns over time.

Figure 7 Comparison of DNN-SGD with ANN, DNN, ANN-PSO and ANN-SGD for rainfall runoff modelling (see online version for colours)

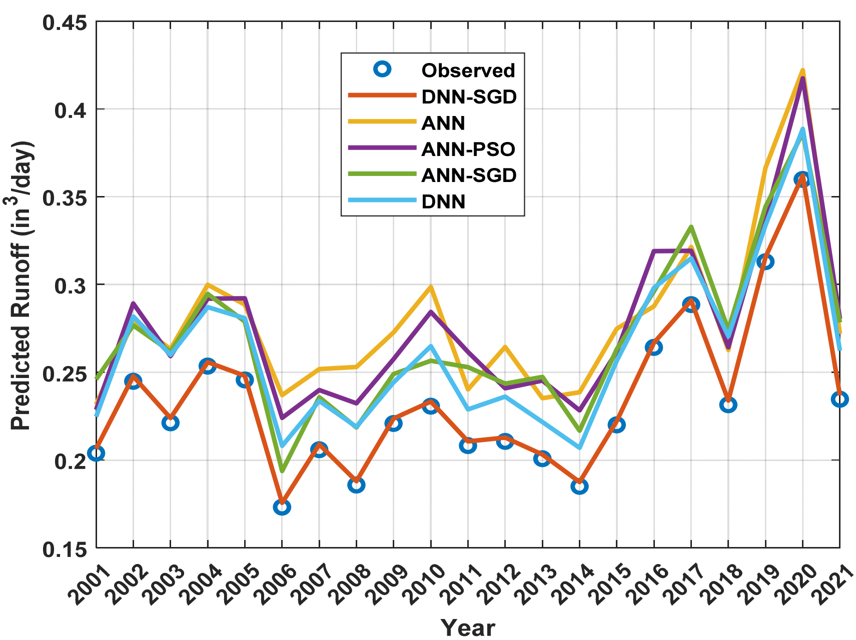

Overall, the proposed DNN-SGD model consistently performs well and provides accurate runoff predictions, with small differences from the actual values across the years. The performances of other comparison models in most cases are not significant. The use of SGD as the optimisation algorithm have contributed to the model's success in finding good parameter values and minimise the errors during training. The highest predicted runoff was observed in 2020, while the lowest predicted runoff was observed in 2006.

4 Conclusions and future scope

In this study, the performance of rainfall runoff modelling was analysed in the Sub Basin (Brahmaputra lower) of the Brahmaputra River on a yearly scale and weather data are considered for predicting runoff. An evaluation criterion of R^2, RMSE and MSE was also determined by DNN-SGD optimisation on a yearly scale. The performance and prediction of runoff are compared with ANN, DNN, ANN-PSO and ANN-SGD. The finding of this study is given below.

- The runoff is determined and predicted by DNN-SGD, ANN, DNN, ANN-PSO and ANN-SGD, and runoff prediction by DNN-SGD optimisation has better prediction with R = 0.99998 than ANN, DNN, ANN-PSO and ANN-SGD methods.
- The proposed DNN-SGD model outperforms all other methods in this comparison, achieving the lowest 0.000507 MSE, 0.002252 RMSE, and the highest 0.9938 R^2 value.
- The highest observed runoff in 2020 and the lowest observed runoff in 2006 were obtained from the prediction of the DNN-SGD optimisation model.
- Engineers and planners use this runoff modelling for various reasons such as awareness for flood mitigation, possible flood events, disaster management, flood insurance, embankments and dykes construction, etc. Also used for flood zone identification, flood management systems and water management systems for flood control.

While the proposed work shows promising results in improving the accuracy of runoff prediction using the DNN-SGD model, it is essential to acknowledge of its drawback to provide a comprehensive perspective for future research. The proposed DNN-SGD model's success in the Brahmaputra River Sub Basin. But it raises questions about its transferability to other regions with different hydrological characteristics. It is crucial to assess the model's performance in various geographical areas and climatic conditions to determine its applicability. To overcome this drawback, future research should focus on the following: Collecting more extensive and diverse datasets from multiple regions will improve the model's robustness and ensure its applicability in various hydrological settings. By addressing this limitation, the proposed work further improve the reliable and accurate rainfall-runoff prediction models for water resource management.

References

Adnan, R.M., Petroselli, A., Heddam, S., Santos, C.A.G. and Kisi, O. (2021a) 'Comparison of different methodologies for rainfall-runoff modeling: machine learning vs. conceptual approach', *Natural Hazards*, Vol. 105, pp.2987–3011.

Adnan, R.M., Petroselli, A., Heddam, S., Santos, C.A.G. and Kisi, O. (2021b) 'Short term rainfall-runoff modelling using several machine learning methods and a conceptual event-based model', *Stochastic Environmental Research and Risk Assessment*, Vol. 35, No. 3, pp.597–616.

Ahmed, I.A., Dutta, D.K., Baig, M.R.I., Roy, S.S. and Rahman, A. (2021) 'Implications of changes in temperature and precipitation on the discharge of Brahmaputra River in the urban watershed of Guwahati, India', *Environmental Monitoring and Assessment*, Vol. 193, pp.1–21.

Barbulescu, A., Barbes, L. and Dumitriu, C.S. (2021) 'Assessing the water pollution of the Brahmaputra River using water quality indexes', *Toxics*, Vol. 9, No. 11, p.297.

Ben Khélifa, W. and Mosbahi, M. (2021) 'Modeling of rainfall-runoff process using HEC-HMS model for an urban ungauged watershed in Tunisia', *Modeling Earth Systems and Environment*, pp.1–10.

Bunganaen, W., Frans, J.H., Seran, Y.A., Legono, D. and Krisnayanti, D.S. (2021) 'Rainfall-runoff simulation using HEC-HMS model in the Benanain Watershed, Timor Island', in *J. Civ. Eng. Forum*, Vol. 7, No. 3, p.359.

Chen, J., Zheng, H., Xiong, H., Chen, R., Du, T., Hong, Z. and Ji, S. (2021) 'FineFool: a novel DNN object contour attack on image recognition based on the attention perturbation adversarial technique', *Computers & Security*, Vol. 104, p.102220.

Chiang, S., Chang, C.H. and Chen, W.B. (2022) 'Comparison of rainfall-runoff simulation between support vector regression and HEC-HMS for a rural watershed in Taiwan', *Water*, Vol. 14, No. 2, p.191.

Deb, P. and Kiem, A.S. (2020). 'Evaluation of rainfall-runoff model performance under non-stationary hydroclimatic conditions', *Hydrological Sciences Journal*, Vol. 65, No. 10, pp.1667–1684.

Dietrich, M., Best, K.B., Raff, J.L. and Ronay, E.R. (2020) 'A first-order geochemical budget for suspended sediment discharge to the Bay of Bengal from the Ganges-Brahmaputra river system', *Science of The Total Environment*, Vol. 726, p.138667.

Elagca, A. (2022) 'Application of Arc-GIS, HEC-GeoHMS and HEC-HMS in a holistic sense for estimation of rainfall-runoff process: case study over Ballikaya Basin', *Acta Scientiarum. Technology*, Vol. 44, pp.e58360–e58360.

Faouzi, E., Arioua, A., Hssaisoune, M., Boudhar, A., Elaloui, A. and Karaoui, I. (2022) 'Sensitivity analysis of CN using SCS-CN approach, rain gauges and TRMM satellite data assessment into HEC-HMS hydrological model in the upper basin of Oum Er Rbia, Morocco', *Modeling Earth Systems and Environment*, Vol. 8, No. 4, pp.4707–4729.

Gholami, V. and Khaleghi, M.R. (2021) 'A simulation of the rainfall-runoff process using artificial neural network and HEC-HMS model in forest lands', *Journal of Forest Science*, Vol. 67, No. 4, pp.165–174.

Gholami, V. and Sahour, H. (2022) 'Simulation of rainfall-runoff process using an artificial neural network (ANN) and field plots data', *Theoretical and Applied Climatology*, pp.1–12.

Hamdan, A.N.A., Almuktar, S. and Scholz, M. (2021) 'Rainfall-runoff modeling using the HEC-HMS model for the Al-Adhaim river catchment, Northern Iraq', *Hydrology*, Vol. 8, No. 2, p.58.

Ibrahim, A., Zakaria, N., Harun, N. and Hashim, M.M.M. (2021) 'Rainfall runoff modeling for the basin in Bukit Kledang, Perak', in *IOP Conference Series: Materials Science and Engineering*, Vol. 1106, No. 1, p.012033, IOP Publishing.

Jimmy, S.R., Sahoo, A., Samantaray, S. and Ghose, D.K. (2021) 'Prophecy of runoff in a river basin using various neural networks', in *Communication Software and Networks: Proceedings of INDIA 2019*, Springer, Singapore pp.709–718.

Kou, C., Qi, Y., Kang, A., Hu, H. and Wu, X. (2021) 'Spatiotemporal distribution characteristics of runoff-pollutants from three types of urban pavements', *Journal of Cleaner Production*, Vol. 292, p.125885.

Kumar, P. and Sherring, A. (2021) 'Modelling of rainfall and runoff using HEC-HMS in Oghani Micro-watershed of Azamgarh District Uttar Pradesh', *IJCS*, Vol. 9, No. 1, pp.3476–3482.

Lian, H., Yen, H., Huang, J.C., Feng, Q., Qin, L., Bashir, M.A., Wu, S., Zhu, A.X., Luo, J., Di, H. and Lei, Q. (2020) 'CN-China: revised runoff curve number by using rainfall-runoff events data in China', *Water Research*, Vol. 177, p.115767.

Liu, J., Zhou, J., Yao, J., Zhang, X., Li, L., Xu, X., He, X., Wang, B., Fu, S., Niu, T. and Yan, J. (2020) 'Impact of meteorological factors on the COVID-19 transmission: a multi-city study in China', *Science of the Total Environment*, Vol. 726, p.138513.

Liu, L., Luo, D., Wang, L., Huang, Y. and Chen, F. (2020) 'Variability of soil freeze depth in association with climate change from 1901 to 2016 in the upper Brahmaputra River Basin, Tibetan Plateau', *Theoretical and Applied Climatology*, Vol. 142, pp.19–28.

Mao, G., Wang, M., Liu, J., Wang, Z., Wang, K., Meng, Y., Zhong, R., Wang, H. and Li, Y. (2021) 'Comprehensive comparison of artificial neural networks and long short-term memory networks for rainfall-runoff simulation', *Physics and Chemistry of the Earth, Parts A/B/C*, Vol. 123, p.103026.

Molajou, A., Nourani, V., Afshar, A., Khosravi, M. and Brysiewicz, A. (2021) 'Optimal design and feature selection by genetic algorithm for emotional artificial neural network (EANN) in rainfall-runoff modeling', *Water Resources Management*, Vol. 35, No. 8, pp.2369–2384.

Müller, A., Österlund, H., Marsalek, J. and Viklander, M. (2020) 'The pollution conveyed by urban runoff: a review of sources', *Science of the Total Environment*, Vol. 709, p.136125.

NASA (2021) *POWER* [online] https://power.larc.nasa.gov/data-access-viewer/ (accessed September 2022).

Nourani, V., Gökçekuş, H. and Gichamo, T. (2021) 'Ensemble data-driven rainfall-runoff modeling using multi-source satellite and gauge rainfall data input fusion', *Earth Science Informatics*, Vol. 14, No. 4, pp.1787–1808.

Okkan, U., Ersoy, Z.B., Kumanlioglu, A.A. and Fistikoglu, O. (2021) 'Embedding machine learning techniques into a conceptual model to improve monthly runoff simulation: a nested hybrid rainfall-runoff modeling', *Journal of Hydrology*, Vol. 598, p.126433.

Rao, M.P., Cook, E.R., Cook, B.I., D'Arrigo, R.D., Palmer, J.G., Lall, U., Woodhouse, C.A., Buckley, B.M., Uriarte, M., Bishop, D.A. and Jian, J. (2020) 'Seven centuries of reconstructed Brahmaputra River discharge demonstrate underestimated high discharge and flood hazard frequency', *Nature Communications*, Vol. 11, No. 1, p.6017.

Ruder, S. (2016) *An Overview of Gradient Descent Optimization Algorithms*, arXiv preprint arXiv:1609.04747.

Sabaghi, B., Shafai Bajestan, M. and Aminnejad, B. (2021) 'Uncertainty analysis of rainfall-runoff relationships using fuzzy set theory and copula functions', *Iranian Journal of Science and Technology, Transactions of Civil Engineering*, pp.1–10.

Sezen, C. and Partal, T. (2022) 'New hybrid GR6J-wavelet-based genetic algorithm-artificial neural network (GR6J-WGANN) conceptual-data-driven model approaches for daily rainfall-runoff modelling', *Neural Computing and Applications*, Vol. 34, No. 20, pp.17231–17255.

Sun, J., Wang, X. and Shahid, S. (2020) 'Precipitation and runoff variation characteristics in typical regions of North China Plain: a case study of Hengshui City', *Theoretical and Applied Climatology*, Vol. 142, pp.971–985.

Suresh, A., Chanda, A., Rahaman, Z.A., Kafy, A.A., Rahaman, S.N., Hossain, M.I., Rahman, M.T. and Yadav, G. (2022) 'A geospatial approach in modelling the morphometric characteristics and course of Brahmaputra river using sinuosity index', *Environmental and Sustainability Indicators*, Vol. 15, p.100196.

Tsering, T., Sillanpää, M., Sillanpää, M., Viitala, M. and Reinikainen, S.P. (2021) 'Microplastics pollution in the Brahmaputra River and the Indus River of the Indian Himalaya', *Science of the Total Environment*, Vol. 789, p.147968.

Wang, J., He, G., Fang, H. and Han, Y. (2020) 'Climate change impacts on the topography and ecological environment of the wetlands in the middle reaches of the Yarlung Zangbo-Brahmaputra River', *Journal of Hydrology*, Vol. 590, p.125419.

Xu, Y., Hu, C., Wu, Q., Jian, S., Li, Z., Chen, Y., Zhang, G., Zhang, Z. and Wang, S. (2022) 'Research on particle swarm optimization in LSTM neural networks for rainfall-runoff simulation', *Journal of Hydrology*, Vol. 608, p.127553.

Xue, M., Wu, Z., He, C., Wang, J. and Liu, W. (2020) 'Active DNN IP protection: a novel user fingerprint management and DNN authorization control technique', in *2020 IEEE 19th International Conference on Trust, Security and Privacy in Computing and Communications (TrustCom) IEEE*, pp.975–982.